

Investigation of the Roughness Strip Effects on the Separation-Induced Transition with the $\gamma - \widetilde{Re}_{\theta t}$ Transition Model on a High-Lift Low-Pressure Turbine Rotor Blade at Steady Conditions

J.R. Llobet - J. Babajee - T. Arts

Turbomachinery and Propulsion Department
von Karman Institute for Fluid Dynamics
1640 Rhode-Saint-Genèse, Belgium.

(juanrallg@gmail.com, jayson.babajee@vki.ac.be, tony.arts@vki.ac.be)

ABSTRACT

The investigation of a specific CFD approach for studying the effect of roughness strips mounted on the suction side of a low-pressure turbine (LPT) blade is presented. The tests are carried out using the ONERA CFD code *elsA*. The test case is a cascade with a high pitch-to-chord ratio ($g/c = 0.95$) of the widely used T106C high-lift (HL) LPT blade. The *Chimera Technique* is used to introduce the roughness strips geometry in the mesh. Two different geometries are tested: a “wavy wire” and a “straight wire”. The Langtry & Menter transition model and the Abu-Ghannam & Shaw transition criterion are used, and their suitability for this purpose is assessed. The CFD results are compared with the experimental data obtained at the von Karman Institute (VKI) in the framework of the TATMo and UTAT European programmes. The tests are carried out at an outlet isentropic Reynolds number ($Re_{2,is}$) ranging from 80000 to 185000, at a constant outlet isentropic Mach number (0.65) and inlet turbulent intensity (0.9%) in order to match the already existing experimental results.

NOMENCLATURE

Acronyms

A&S	=	Abu-Ghannam & Shaw trans. crit.
HL	=	High Lift
LPT	=	Low Pressure Turbine
L&M	=	Langtry & Menter trans. model

Symbols

E	=	Destruction term of transport eq.
$\frac{g}{c}$	=	Pitch to chord ratio
h_r	=	Strip height
M	=	Mach number

P	=	Production term of transport eq.
Re	=	Reynolds number
Re_ν	=	Vorticity Re
Re_θ	=	Momentum thickness Re
$\widetilde{Re}_{\theta t}$	=	Local transition Re_θ
s	=	Curvilinear abscissa
s_0	=	Suction side curvilinear length
Tu	=	Turbulence intensity [%]
U	=	Velocity
y	=	Wall distance

Greek Symbols

δ	=	Boundary layer thickness
γ	=	Intermittency
μ	=	Viscosity
μ_l	=	Laminar viscosity
μ_t	=	Turbulent viscosity
ν	=	Kinematic viscosity
θ	=	Momentum thickness

ρ	=	Density
σ	=	Transport eq. diffusion coef.
ζ	=	Kinetic losses [%]: $1 - \left[\frac{V_2}{V_{2, is}} \right]^2$

Subscripts

is	=	Isentropic
t	=	Transition onset
1	=	Inlet condition
2	=	Outlet condition
∞	=	Boundary layer edge condition

INTRODUCTION

One of the major concerns in the aircraft jet engine design is the weight reduction. The largest component, weighting up to 30% of the overall engine mass, is the LPT. The current tendency in gas turbine design is to reduce the weight of the LPT by diminishing the number of blades per stage. This leads to an increase in blade loading, which can present a severe drawback, specially for high-lift blades: further increase in blade loading can lead to boundary layer separation and a high increase of the losses (Sieverding, 1985). Due to the high altitude during cruise, the Reynolds number value in the LPT drops. This increases the risk of separation due to the delay in the boundary layer transition from laminar to turbulent. In order to further reduce the number of blades, special devices meant to trigger transition on the suction side are required to avoid a heavy separation. The simplest and among the most promising elements presently considered to trigger boundary layer transition are the roughness strips (Zhang et al., 2006). These are passive devices consisting of a thin roughness strip located along the span over the blade suction side. It has been found that the implementation of these devices reduces the losses at very low Reynolds number. However, their effect can be disadvantageous at higher Reynolds number depending on the turbulence level and incoming wakes frequency (Himmel et al., 2009) (Sieverding and Bagnera, 2004) (Himmel and Hodson, 2009). The assessment of roughness strips for a certain application requires to take into account a wide range of parameters, such as their shape, height, width and location, along with the different flow conditions such as Reynolds number, Mach number, turbulence intensity and incoming wakes (Himmel et al., 2009). This reinforces the interest of a reliable CFD methodology that would allow to drastically reduce the required experimental test campaigns. Currently, two main approaches can be found in the literature. One uses correlations in order to simulate the effect of the strip without meshing the real geometry. These models require less mesh refinement, but may present a misbehaviour of the flow especially around the strip location (UTAT and TATMo programmes). In addition, different models are required for different strip geometries and most would need thorough experimental studies to characterize them. The other methodology consists in introducing the strip geometry in the mesh. This requires a substantial mesh refinement

around the strip location, but a reliable methodology of this kind would allow to study the potential of any strip at relatively low cost before performing an experimental validation of the results. This paper tackles this topic by studying the validity of using the *Chimera Technique* to introduce the strip geometry in the mesh in combination with the Langtry & Menter transition model (Langtry and Menter, 2009) and the Abu-Ghannam & Shaw transition criterion (Abu-Ghannam and Shaw, 1980). The CFD functionalities used for this investigation were implemented by the *elsA* team (Content and Houdeville, 2011) (ONERA, 2010).

COMPUTATIONAL ENVIRONMENT

CFD Code and Methodology

The CFD software used is the *elsA* code (Cambier, 1999), developed by ONERA. It is dedicated to numerical simulation of compressible, viscous, mono-species, steady and unsteady flows, on three-dimensional multi-block structured meshes.

A steady RANS approach with the Menter $k - \omega$ SST turbulence model coupled to a transition criterion or model is used in the presented study (Babajee and Arts, 2012a) (Babajee and Arts, 2012b). The “Roe” scheme with second order accuracy in space and the “backward Euler” integration scheme with first order accuracy in time are used. The convergence was assessed from the kinetic losses, the mass flow and the aft suction side wall static pressure distributions. Moreover, the usual 3 orders of magnitude drop of the residuals was chosen.

Chimera Technique

The Chimera technique is used to simplify the meshing of complicated geometries or the addition of new features in the mesh. It allows overlapping different mesh blocks in order to add new features to an already existing meshed geometry (Brezzi et al., 2001). This method consists of transferring the solution from overlapping grids by interpolation. Three different zone statuses are created for the overlapping:

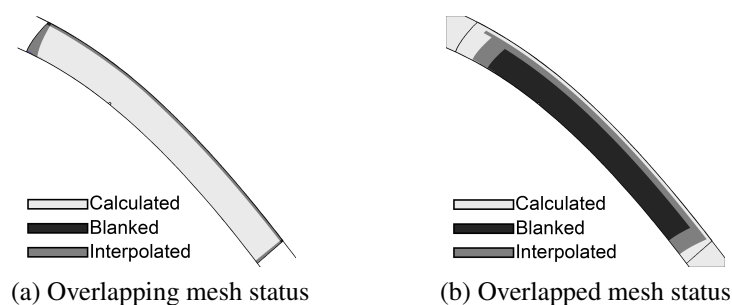


Figure 1: Zones status at overlapping.

- Blanked zone: This is a non-calculated zone. It is located in the overlapped mesh

(Fig. 1b). The calculation of this zone is performed in the corresponding area of the overlapping mesh. This region is where the features of the overlapping mesh substitute the features of the overlapped mesh. In the present case, the overlapped mesh corresponds to the smooth blade, whereas the overlapping mesh contains the strip geometry.

- Interpolated zone: This zone is situated at the limit of the overlapped and overlapping meshes. It is where the information is transferred between meshes (Fig. 1). The overlapping mesh will get its boundary conditions through this area (Fig. 1a). In the same way, the overlapped mesh will retrieve the information of the flow inside the overlapping zone through these regions (Fig. 1b).
- Calculated zone: This zone is calculated normally.

Abu-Ghannam & Shaw Transition Criterion (A&S)

This transition criterion was developed by Abu-Ghannam and Shaw (1980) mainly for “natural” and “by-pass” transition. It predicts the start of transition as a function of the turbulence level and a pressure-gradient parameter from Equations 1 and 2.

$$Re_{\theta S} = 163 + \exp \left\{ F(\lambda_{\theta}) - \frac{F(\lambda_{\theta})}{6.91} Tu \right\} \quad (1)$$

$$\lambda_{\theta} = \frac{\theta^2}{\nu} \frac{\partial U_{\infty}}{\partial s} \quad (2)$$

Then, it switches on the numerical intermittency at the position where the criterion is met.

Langtry & Menter Transition Model (L&M)

The transition model proposed by Langtry and Menter (2009) is based on the van Driest and Blumer’s vorticity Reynolds number concept (Eq. 3). It allows to link the boundary layer quantities with a correlation for the transition onset Reynolds number thanks to Eq. 4.

$$Re_{\nu} = \frac{\rho y^2}{\mu} \left| \frac{\partial u}{\partial y} \right| \quad (3)$$

$$Re_{\theta} = \frac{\max(Re_{\nu})}{2.193} \quad (4)$$

This model gets rid of the need of integrating the boundary layer velocity profile along “computation lines”, providing a purely local transition model.

It is built on the transport equation of the numerical intermittency γ (Eq. 5), which can be triggered locally, and the transport equation of $\widetilde{Re}_{\theta,t}$ (the “transition onset” momentum thickness Reynolds number) (Eq. 6).

$$\frac{\partial(\rho\gamma)}{\partial t} + \frac{\partial(\rho U_j \gamma)}{\partial x_j} = P_\gamma - E_\gamma + \frac{\partial}{\partial x_j} \left[\left(\mu + \frac{\mu_t}{\sigma_f} \right) \frac{\partial \gamma}{\partial x_j} \right] \quad (5)$$

$$\frac{\partial(\rho \widetilde{Re}_{\theta,t})}{\partial t} + \frac{\partial(\rho U_j \widetilde{Re}_{\theta,t})}{\partial x_j} = P_{\theta t} + \frac{\partial}{\partial x_j} \left[\sigma_{\theta t} (\mu + \mu_t) \frac{\partial \widetilde{Re}_{\theta,t}}{\partial x_j} \right] \quad (6)$$

The numerical intermittency function is coupled with the SST $k - \omega$ turbulence model, which allows to turn on the production term of the turbulent kinetic energy downstream of the transition onset.

The formulation for the numerical intermittency was extended in order to account for the rapid onset of transition caused by the separation of the laminar boundary layer (Langtry, 2006) (Langtry and Menter, 2009) (Malkiel and Mayle, 1996).

Blade Mesh and Strip Addition

The procedure described in this paper consists of the addition of the roughness strip geometry to the smooth blade mesh using the *Chimera Technique*, i.e., using the mesh of the smooth blade and overlapping a specific mesh block containing the roughness strip geometry.

Smooth Blade Mesh

The baseline blade used for this study is the widely used T106C blade mounted in a linear cascade. This is an aft-loaded HL-LPT blade. The pitch-to-chord ratio of the cascade is set to ($g/c = 0.95$). The T106C blade mesh used is a truncated 3D mesh. It provides the simulation of an infinite blade by setting symmetry boundary conditions on its spanwise limits. This allows isolating the studied phenomena from secondary losses or tip leakage. The mesh consists of 5 blocks (Fig. 2e). It was formerly tested in order to assess its grid independence properties (Babajee and Arts, 2012a). The lowest value for the orthogonality is 31.1 deg, and the highest expansion ratio is of 1.71. The y^+ value is kept below 0.2 for all cases along the whole blade surface.

Roughness Strip Mesh

The roughness strip geometries consist of a straight wire and a wavy wire. The wavy wire has a height of 0.2 mm and a width of 2 mm. It is located between $\frac{S}{S_0} = 0.52 - 0.54$. The straight wire (Fig. 2c) has a diameter of 0.2 mm and its centre is located at $\frac{S}{S_0} = 0.513$.

The most relevant parameter of a strip was shown to be its height (TATMo programme). Therefore, as a first approximation for the wavy wire, only a 2D cut will be

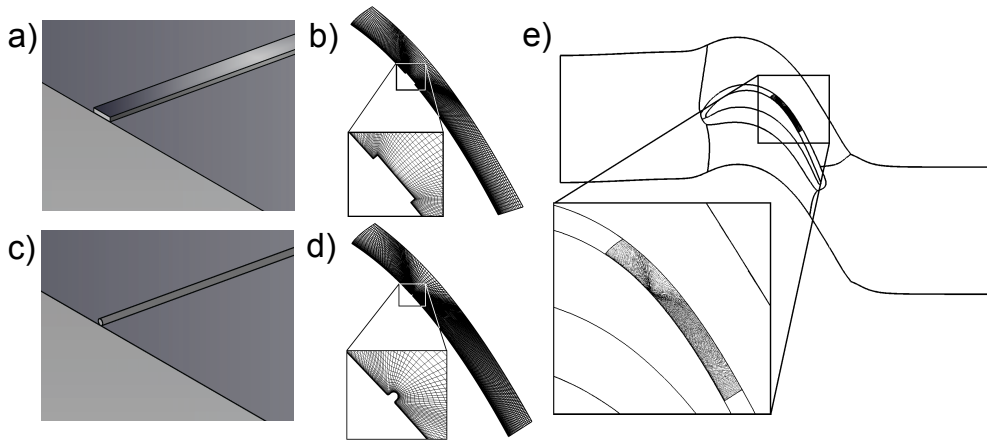


Figure 2: Strips geometry, mesh and overlapping location.

modeled, with a shape of a straight step (Figs. 2a and 2b).

The straight wire geometry is cylindrical (Fig. 2c). However, the effect of the glue, used for its implementation, is not negligible. The zone contiguous with the blade is modelled in order to introduce the effect of the glue on the final shape. In addition, this feature facilitates the meshing of the block in the surroundings of the strip (Fig. 2d). A mesh independence study was carried out for the mesh block containing the roughness strip geometry. The considered parameters were the length of the mesh upstream and downstream of the strip location and the density of the mesh. It is advisable that the upstream and downstream lengths of the mesh cover the recirculation zones generated by the strip. The upstream length can be relatively small, as the recirculation bubble size on the front part of the strip is of the order of the strip height (h_r). On the contrary, the recirculation bubble downstream of the strip was found to be around $50h_r$ to $100h_r$.

However, it is advisable to extend the length of the mesh much more in order to allow a good area of overlapping between meshes. This allows the *Chimera technique* to interpolate far from the area of interest. Following this reasoning, the selected upstream length is $50h_r$. The selected downstream length is $100h_r$ for $Re_{2, is}$ ranging from 120000 to 185000, and $130h_r$ for $Re_{2, is}$ ranging from 80000 to 100000. The length of the normal direction to the blade surface is selected to match the dimension of the O-mesh of the smooth blade.

The lowest orthogonality for the employed meshes (Figs. 2b and 2d) is of 33.08 degrees and the maximum expansion ratio is 1.47. They contain around 7000 nodes per layer. The value of y^+ is kept below 0.1 for all cases along the whole blade surface. The overlapping location of these blocks is illustrated in Fig. 2e.

RESULTS

Chimera Technique Assessment

Several tests were carried out in order to assess the reliability of the *Chimera Technique*. Two different interpolating options for the overlapping zones were tested to compare the obtained results. The first one is the *Implicit hole cutting*. It is a cell selection process where only the “best” cells located in a multiple overlapping region are used for the calculation. The algorithm selects as the most suitable cells the ones that present a better value for the criterion parameter. By these means, the algorithm selects the cells to be calculated (overlapping zone) and the blanked cells (overlapped zone). The second one is the *Patch assembly*. It is based on the designation of different priorities for the multiple overlapping meshes. For this method, the user has to define the higher priority to the mesh where the calculation must be done. By these means, the algorithm automatically assigns the blanking zones to avoid calculation in the overlapped mesh and forces it to be done in the overlapping one. Also, one test involving only the baseline smooth blade configuration with the standard 5-block on one side, and the 5-block mesh associated to an overlapping block on the other side was carried out in order to assess the transfer of information of the *Chimera Technique*. These analyses allowed to confirm that the effect on the results of the *Chimera Technique* is none or negligible according to the comparison done on the blade pressure distribution and on the downstream wakes.

These tests also allowed to quantify the increase in computational cost due to the use of this technique. The strip block cells constitute a 15% increase with respect to the basic mesh. This, together with the interpolation required in certain regions, increased the computational time and memory by about 30%.

Straight Step (2D wavy wire) Results

The blade isentropic Mach number distributions over the suction side for $Re_{2, is} = 100000$ and $Re_{2, is} = 160000$ cases are presented in Fig. 3. In addition to the CFD results, the experimental data obtained, within the frame of the UTAT programme at the VKI, are shown. The dotted lines represent the location of the strip. The L&M results show a good agreement with the experiments. The blade isentropic Mach number peak generated by the strip and the subsequent separation bubble length are very accurately predicted. On the contrary, the A&S results show much less accurate results for these features.

This is caused by the different transition onset location obtained with both methods. Fig. 4a shows the predicted locations for both approaches, along with the experimental results and the strip location. The transition location onset is defined by the viscosity ratio ($\frac{\mu_t}{\mu_l}$) from the CFD predictions and takes place where this value reaches 1. Concerning the experimental information, one can assess it from the RMS of the hot-films signal. The data obtained with L&M present a very accurate transition onset location,

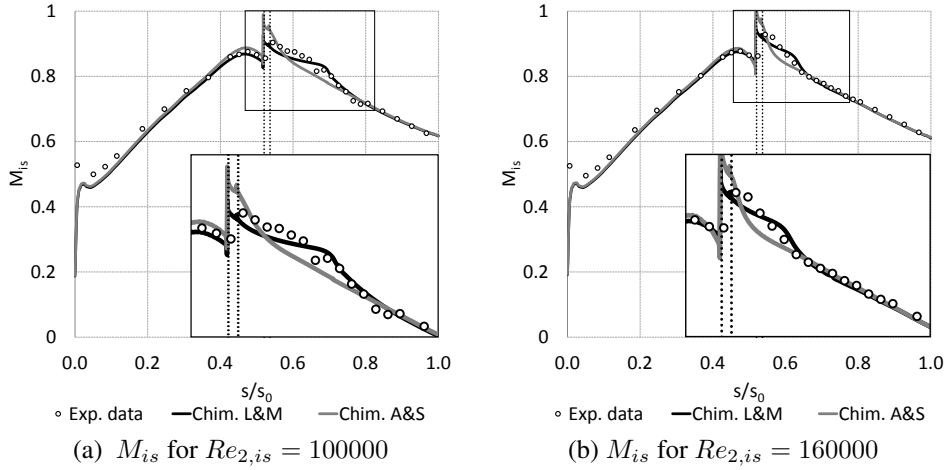


Figure 3: M_{is} distribution for the $Re_{2,is} = 100000$ and $Re_{2,is} = 160000$ cases.

whereas the results obtained with A&S show transition onset locations much more upstream than expected. The early transition predicted by A&S accounts for the inaccu-

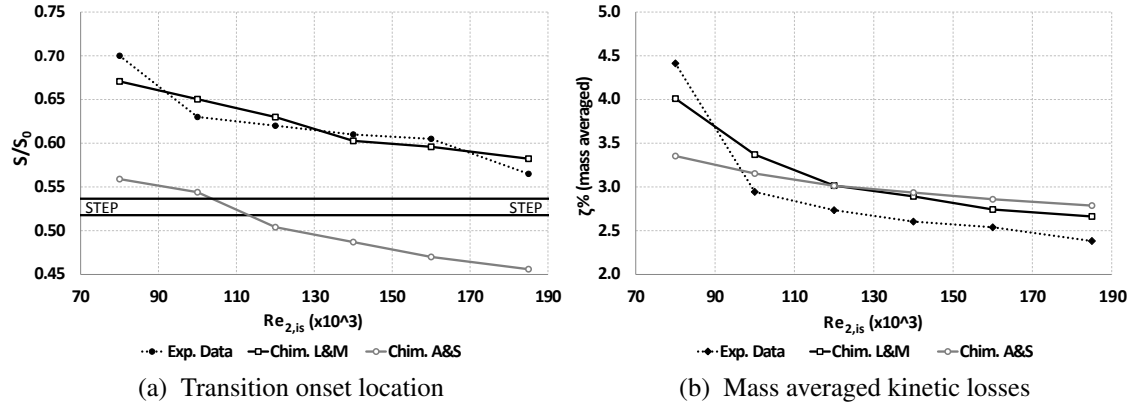


Figure 4: Transition onset location and kinetic losses for the straight step case

racy of the method. The presence of a turbulent boundary layer upstream or close to the strip location and/or the velocity peak location insures the further development of a fully turbulent boundary layer which is less prone to separation in the diffusing part of the blade.

Moreover, the transition onset location highly affects the obtained predictions for the kinetic losses. The results provided by the L&M calculations follow the trend of the kinetic losses relatively well for the studied $Re_{2,is}$ range, as can be seen in Fig. 4b. On the contrary, the same plot shows the misbehaviour of the results obtained with A&S, which do not present the step increase in kinetic losses at very low $Re_{2,is}$. Indeed, at

very low $Re_{2,is}$, the transition is predicted too early and provides lower losses due to the non-existence of a separation bubble. At higher $Re_{2,is}$, the increase in wall shear stress due to the increased length of the turbulent boundary layer becomes more important and the kinetic losses are over-predicted. Even though the transition onset predictions are not at the same location between the A&S and the L&M models, the losses are comparable at mid and high $Re_{2,is}$ but diverge at low $Re_{2,is}$. This might be explained by the fact that at mid and high $Re_{2,is}$, the separation bubble is still short and consequently does not affect the boundary layer evolution whereas at low $Re_{2,is}$, the separation bubble has a more pronounced effect on the boundary layer evolution. Consequently, the predicted losses are affected.

Straight Wire Results

The blade isentropic Mach number distributions over the suction side for $Re_{2,is} = 100000$ and 160000 are presented in Fig. 5. Along with the CFD results, the experimental data obtained within the frame of the TATMo programme at the VKI are shown as well. In this case, the dotted line represents the location of the centre of the wire. For the straight wire cases, the results obtained with A&S and the L&M present similar

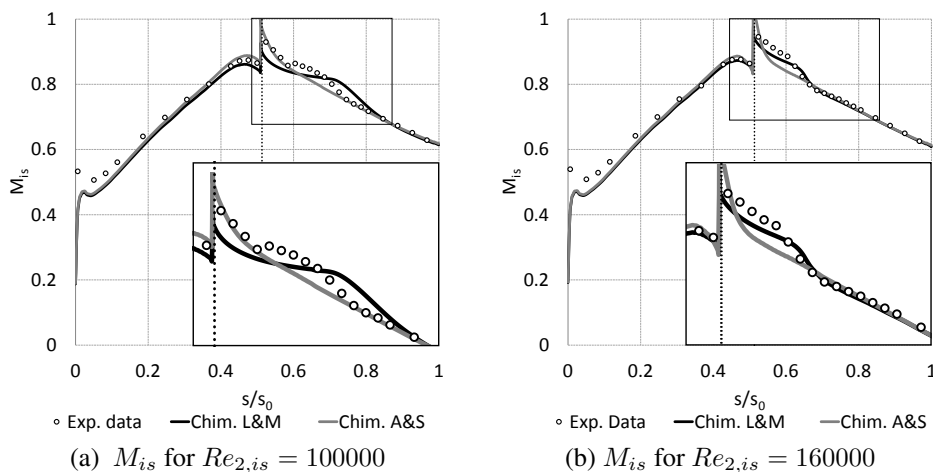


Figure 5: M_{is} distribution for the $Re_{2,is} = 100000$ and $Re_{2,is} = 160000$ cases.

behaviour in comparison to the straight step cases (Figs. 6a and 6b). Unfortunately, experimental information on the transition onset were not available for this configuration. The trend of the losses is still relatively well predicted (Fig. 6b). However, the numerical predictions at low $Re_{2,is}$ are higher than the experimental results. The explanation might be a delay in the transition onset location that could lead to a longer laminar boundary layer associated to a stronger separation bubble. This affects the bubble height and consequently the wake profile. In addition, the M_{is} distribution is highly affected by this fact (Fig. 5a). This transition model has not been extended for specific

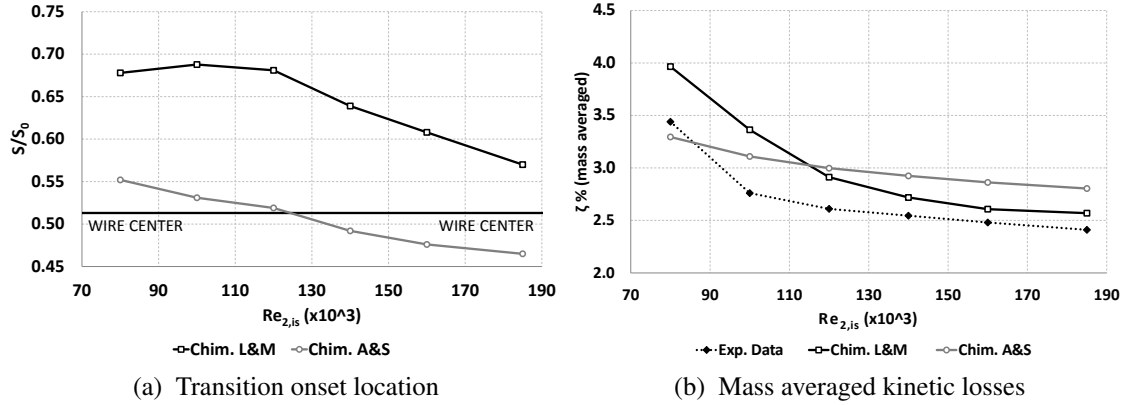


Figure 6: Transition onset location and kinetic losses for the straight wire case

use on roughness strips and yet, very satisfactory results have been obtained for the majority of the studied cases. The fact that it was modified for separated flow transition provides very accurate transition length predictions (Babajee and Arts, 2012a) (Babajee and Arts, 2012b). However, further work could be directed to improve this transition model for the specific case of roughness strips. The value of the critical momentum thickness Reynolds number could be reduced in order to move upstream the transition onset location in the trip wire cases.

Probably, the main difficulty for L&M to obtain valid results over the whole range of $Re_{2, is}$ is that the effect of the strip takes place far below from the boundary layer edge, usually around $\frac{y}{\delta} = 0.1$. The $Re_{\theta t}$ value is calculated at the edge of the boundary layer, and then diffused inside the boundary layer as a local $\widetilde{Re}_{\theta t}$ value. As the effect of the strip is far from the $Re_{\theta t}$ calculation point, for some conditions this diffusion may be too low to provide a proper transition onset location. A mechanism to activate the production term of turbulent kinetic energy directly where the roughness strip is affecting the flow could improve the range of validity of the model for roughness strip calculations. The significant increase of the vorticity Reynolds number (Re_ν) or the severe variation of vorticity modulus generated by the strip inside the boundary layer could be used as triggering parameter for the intermittency.

Regarding A&S, the results obtained with this criterion are not satisfactory. The transition onset location is found too upstream for all the studied cases. Unlike L&M, A&S takes into account only the transition criterion at the boundary layer edge. The momentum thickness is increased in the surroundings of the strip. Due to this, the transition criterion is satisfied at the strip location or even slightly upstream, setting the whole boundary layer as turbulent at this location and providing poor agreement with the experimental results.

Concerning the flow around the trip wire configurations, the L&M model provides

a better representation of the separation occurring downstream. Indeed, the extension of the separation bubble is varying with the working conditions due to the more gradual evolution of the transition (with the intermittency) in the L&M model. Therefore, one can conclude that the physics is better represented with the L&M model in comparison to the A&S criterion.

CONCLUSIONS

The use of the *Chimera Technique* to introduce the roughness strip geometry in the mesh, combined with the Langtry & Menter transition model and the Abu-Ghannam & Shaw transition criterion has been assessed.

The *Chimera Technique* has shown to be useful to simplify the meshing of different strip geometries, as only the surroundings of the strip need to be generated. The performed tests allowed to conclude that the final solution is not affected by the use of this technique.

A&S has shown to provide poor agreement with the experimental results for roughness strips. It showed a tendency to predict the transition onset location severely more upstream than expected. This tendency caused the over-prediction of the M_{is} peak and the inability to predict the separation bubble downstream of the strip. On the contrary, despite L&M was not formulated for roughness strips, it shows its ability to predict accurate transition onset location and transition length for most of the studied cases. Moreover, it has the potential to correctly predict the physics of the separation bubble downstream of the trip wire. The blade M_{is} distribution is very accurately retrieved and the losses present good agreement with the experimental data. It presented some misbehaviour only for the straight wire strip geometry at very low $Re_{2,is}$ values.

The use of the *Chimera Technique* along with the Langtry & Menter transition model therefore presents a strong potential for its use in CFD calculations for roughness strips.

ACKNOWLEDGEMENTS

The experimental results reported in this work were obtained within the European research projects UTAT (GRD1-2001-40192) and TATMo (AST5-CT-2006-030939). The authors acknowledge the permission to publish this paper.

REFERENCES

- Abu-Ghannam, B.J. and Shaw, R. (1980). "Natural Transition of Boundary Layers - The effects of Turbulence, Pressure Gradient and Flow History". *Journal of Mechanical Engineering Science*, 22:213-228.
- Babajee, J. and Arts, T. (2012a). "Investigation of the Laminar Separation-Induced Transition with the $\gamma - \widetilde{Re}_{\theta t}$ Transition Model on Low-Pressure Turbine Rotor Blades at Steady Conditions". ASME Turbo Expo 2012: Power for Land, Sea and Air, GT2012-68687, Copenhagen, Denmark.
- Babajee, J. and Arts, T. (2012b). "Investigation of the Laminar Separation-Induced Tran-

sition with the $\gamma - \widetilde{Re}_{\theta t}$ Transition Model on one Very High-Lift Low-Pressure Turbine (T2) and one Engine-like Scale Low-Pressure Turbine (TX) Rotor Blades at Steady Conditions and Freestream Turbulence”. 47th Applied Aerodynamics Symposium, Paris, France.

Brezzi, F., Lions, J. and Pironneau, O. (2001). “Analysis of a Chimera method”. *Comptes Rendus de l’Académie des Sciences-Series I-Mathematics*, 332-7:655-660.

Cambier, L. (1999). “The elsA project”. First ONERA-DLR Aerospace Symposium, Paris, France.

Content, C. and Houdeville, R. (2010), “Application of the γ - R_{θ} laminar-turbulent transition model in Navier-Stokes computations”, AIAA 40th Fluid Dynamics Conference and Exhibit, AIAA 2010-4445, Chicago, Illinois, USA, June 28 - July 4.

Himmel, C. and Hodson, H. (2009). “Modifying Ultra-High Lift Low Pressure Turbine Blades for Low Reynolds Number Applications”. 12th International Symposium on Unsteady Aerodynamics, Aeroacoustics & Aeroelasticity of Turbomachines, ISUAAAT12, Imperial College London, UK.

Himmel, C.G., Thomas, R.L. and Hodson, H.P. (2009). “Effective Passive Flow Control for Ultra-High Lift Low-Pressure Turbines”. 8th European Turbomachinery Conference, Graz, Austria.

Langtry, R.B. (2006). “A Correlation-Based Transition Model using Local Variables for Unstructured Parallelized CFD codes”. PhD Thesis, Institut für Thermische Strömungsmaschinen und Maschinenlaboratorium Universität Stuttgart.

Langtry, R.B. and Menter, F.R. (2009). “Correlation-Based Transition Modeling for Unstructured Parallelized Computational Fluid Dynamics Codes”. *AIAA Journal* Vol. 47, No. 12.

Malkiel, E. and Mayle, R.E. (1996). “Transition in a Separation Bubble”. *Journal of Turbomachinery*, 118-4:752-759.

Sieverding, C.H. (1985). “Subsonic Turbine Blading Design”. von Karman Institute for Fluid Dynamics, Course Note 124.

Sieverding, C.H. and Bagnera, C. (2004). “Investigation of the Effectiveness of Various Types of Boundary Layer Transition Elements of Low Reynolds Number Turbine Bladings”. ASME Turbo Expo 2004: Power for Land, Sea and Air, GT2004-54103, Viena, Austria.

Zhang, X.F., Vera, M. and Hodson, H. (2006). “Separation and Transition Control on an Aft- Loaded Ultra-High-Lift LP Turbine Blade at Low Reynolds Numbers: Low-Speed Investigation”. *Journal of Turbomachinery*, 128:516-527.

ONERA (2010), Private communication.

TATMo programme (2012), Arts, T., Private communication.

UTAT programme (2012), Arts, T., Private communication.